The Infrared Spectrum of Diazirine, $H_2C^{15}N_2$ Rovibrational Analysis of the ν_3 Fundamental

Jürgen Vogt [1]
Physikalisch-Chemisches Institut der Justus-Liebig Universität Giessen *

Alberto Gambi
Dipartimento di Spettroscopia, Elettrochimica e Chimica Fisica, Università di Venezia, Italy

Z. Naturforsch. **41 a**, 1159–1165 (1986); received June 16, 1986

The mid-infrared spectrum of ^{15}N-labeled diazirine has been recorded using a Fourier transform spectrometer at a resolution of 0.08 cm^{-1}. The ν_3 fundamental at 1452.49 cm^{-1} which essentially corresponds to a symmetric methylene deformation has been analyzed in detail. The rovibrational assignment is given and, using Watson's A-reduced Hamiltonian, the rotational and centrifugal distortion constants for the $\nu_3 = 1$ level could be determined.

Introduction

In recent years diazirine, the only experimentally known cyclic isomer of diazomethane, has been of great interest. With the intention of providing a complete set of molecular constants for the ground and the first excited vibrational states of diazirine, an investigation of this molecule, which presents an unusual molecular structure, has been carried out by means of microwave, millimeter wave [1–4], and Fourier transform infrared spectroscopy [5–8]. The infrared spectra of diazirine and its isotopomers $H_2{}^{13}CN_2$, $H_2C^{15}N_2$, and D_2CN_2 have been recorded in isotopically enriched samples with a Fourier transform spectrometer at a resolution of 0.08 cm^{-1}. For the parent species the rovibrational assignment of the ν_3 fundamental (A-type band, A_1 species, CH_2 deformation), the ν_7 fundamental (B-type band, B_1 species, CN asymmetric stretching) and of the ν_9 fundamental (C-type band, B_2 species, CH_2 rocking) have been carried out [5, 6, 8] developing methods for the rotational assignment and for the analysis of the band structure of this very asymmetric rotor. The ν_3 band of $H_2{}^{13}CN_2$ has also been analyzed [7].

In order to continue the thorough study of this molecule, the infrared spectrum and the rovibrational analysis of the ν_3 fundamental of $H_2C^{15}N_2$, resulting in the determination of the molecular constants for the vibrational state $\nu_3 = 1$, has been carried out and will be reported here.

Experimental Procedures

Isotopically enriched ^{15}N-diazirine was prepared by means of a modification of the method of Ohme and Schmitz, which is described elsewhere [1, 9]. In this case ^{15}N-enriched formamide (Merck, Sharp and Dohme, Canada; 96.2 atomic% ^{15}N) was used as a precursor.

The infrared spectrum of $H_2C^{15}N_2$ was recorded using a Digilab Fourier transform spectrometer FTS-20B in the range 450–3800 cm^{-1} purged with dry nitrogen in order to avoid absorptions due to atmospheric water and carbon dioxide. A HgCdTe (MCT) detector, cooled with liquid nitrogen, was used. In order to obtain a reasonable signal-to-noise ratio at a resolution better than 0.08 cm^{-1}, 600 interferograms were coadded and Fourier transformed. The sample cell was 10 cm long and equipped with KBr windows. The sample pressure was about 2000 Pa.

Calibration was made with HBr lines [10] recorded under the same conditions.

Results and Discussion

The $^{15}N_2$-diazirine molecule belongs to the symmetry point group C_{2v}. The nine fundamental vibra-

[1] Present address: Verein Deutscher Ingenieure, Graf-Recke-Str. 84, D-4000 Düsseldorf 1.

* Heinrich-Buff-Ring 58, D-6300 Giessen.

Reprint requests to Alberto Gambi, Dipartimento di Spettroscopia, Elettrochimica e Chimica Fisica, Università di Venezia, D.D. 2137. I-30123 Venezia (Italy).

0340-4811 / 86 / 0900-1159 $ 01.30/0. – Please order a reprint rather than making your own copy.

C_{2v}	E	C_{2a}	σ_{ab}	σ_{ac}	
A_1	1	1	1	1	T_a
A_2	1	1	−1	−1	R_a
B_1	1	−1	1	−1	T_b, R_c
B_2	1	−1	−1	1	T_c, R_b
Γ_{3N}^{tot}	15	−1	3	3	
Γ_{spin}^{tot}	16	4	8	8	

$$\Gamma_{vib} = 4A_1 \oplus A_2 \oplus 2B_1 \oplus 2B_2$$

Band contour → A-type B-type C-type

$I(^{15}N) = 1/2$; $I(^{1}H) = 1/2$; $I(^{12}C) = 0$; $I_{tot} = 16$

$$\Gamma_{spin} = 9A_1 \oplus A_2 \oplus 3B_1 \oplus 3B_2$$

$K_a K_c$	Γ_{rot}	Weight
ee	A_1	6
eo	A_2	6
oe	B_1	10
oo	B_2	10

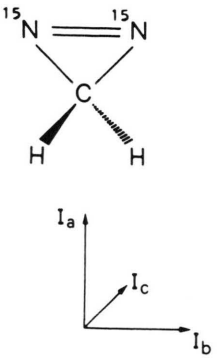

Fig. 1. Symmetry information for $^{15}N_2$-diazirine.

Table 1. Fundamental vibrations of $^{15}N_2$-diazirine.

Symmetry species	Mode	Approximate description	cm^{-1}
A_1	ν_1	sCH stretch	3015.4[a]
	ν_2	NN stretch	1585.2[a]
	ν_3	CH_2 deformation	1452.49
	ν_4	sCN stretch	973.5
A_2	ν_5	CH_2 twist	[959][b]
B_1	ν_6	CH_2 wag	967.2
	ν_7	aCN stretch	786.8
B_2	ν_8	aCH stretch	3131.6
	ν_9	CH_2 rock	1123.7

[a] Perturbed by Fermi resonance. [b] Estimated value.

tions and their symmetry species are $4A_1(\nu_1-\nu_4)$, $A_2(\nu_5)$, $2B_1(\nu_6,\nu_7)$, and $2B_2(\nu_8,\nu_9)$. In Fig. 1 the correlation between the symmetry species of the vibrational irreducible representation and the band contour is given. The spin statistics for the rovibrational levels are also shown (cf. similar table for parent species in [5]).

Figure 2 shows a survey spectrum of $^{15}N_2$-diazirine recorded at low resolution between 600 and 3400 cm^{-1}. The A- and C-type bands exhibit the typical PQR envelop, while the B-type bands present two peaks on either side of the band center (PQQR envelop).

In Table 1 the fundamental vibrations and their descriptions are reported. For the $\nu_5(A_2)$ mode, which is infrared inactive, there are no experimental data; the value listed is deduced from the vibrational analysis of all the substituted species [11]. Since the lowest fundamental is around 800 cm^{-1}, the spectrum is free at least up to 1600 cm^{-1} from overtone and combination bands. The spectrum in Fig. 2 shows the strong Fermi resonance between ν_2 and $2\nu_7$ at 1600 cm^{-1}, and at 3000 cm^{-1} the interaction due to the Fermi resonance of the ν_1, $\nu_2+\nu_3$, and $2\nu_7+\nu_3$ bands.

The region covered by the rovibrational structure of the ν_3 band is shown in Figure 3. Since a precursor enriched to 96.2% in ^{15}N was used for the preparation, the resulting isotopic distribution is 92.5% $H_2C^{15}N_2$, 7.3% $H_2C^{14}N^{15}N$ and about 0.1% of $H_2C^{14}N_2$, so that it was impossible to detect the spectrum of the main isotropic species. However the spectrum exhibits a strong unresolved Q-branch at 1456.4 cm^{-1}, which is evidently the Q-branch of the mixed isotopomer $H_2C^{14}N^{15}N$.

For the numerical analysis of the rovibrational transitions both the ground and the excited state levels were fitted to Watson's A-reduced rotational Hamiltonian [12] in the I^r representation:

$$\begin{aligned}\mathbf{H}_{rot} = {} & 1/2(B+C)\,\mathbf{P}^2 + [A - 1/2(B+C)]\,\mathbf{P}_a^2 \\ & - \Delta_J \mathbf{P}^4 - \Delta_{JK}\mathbf{P}^2\mathbf{P}_a^2 - \Delta_K \mathbf{P}_a^4 + H_{JK}\mathbf{P}^4\mathbf{P}_a^2 \\ & + H_{KJ}\mathbf{P}^2\mathbf{P}_a^4 + [1/2(B-C) - 2\delta_J \mathbf{P}^2]\,(\mathbf{P}_b^2 - \mathbf{P}_c^2) \\ & + [(-\delta_K \mathbf{P}_a^2), (\mathbf{P}_b^2 - \mathbf{P}_c^2)]_+ ,\end{aligned}$$

where $\mathbf{P}$, $\mathbf{P}_a$, $\mathbf{P}_b$, and $\mathbf{P}_c$ are the operators for the total angular momentum and its components, respectively; A, B, and C are the reduced rotational constants for the given vibrational state. Δ_J, Δ_{JK}, Δ_K, δ_J, and δ_K are the quartic and H_{JK}, H_{KJ}, are sextic centrifugal distortion constants.

The assignment of the rovibrational transitions was done with extensive use of modern computed-assisted methods of calculations, simulations, and graphic representation [5, 7]. For this A-type band

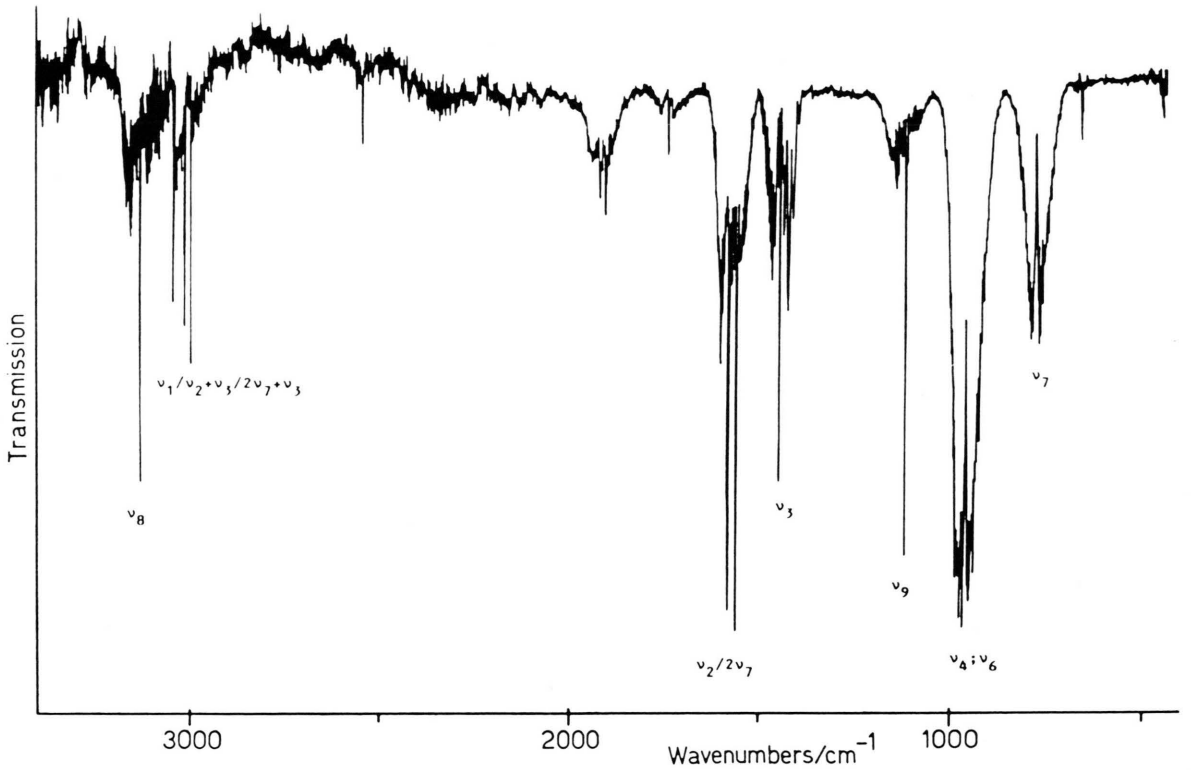

Fig. 2. A survey spectrum (resolution 1.0 cm^{-1}) of $H_2C^{15}N_2$.

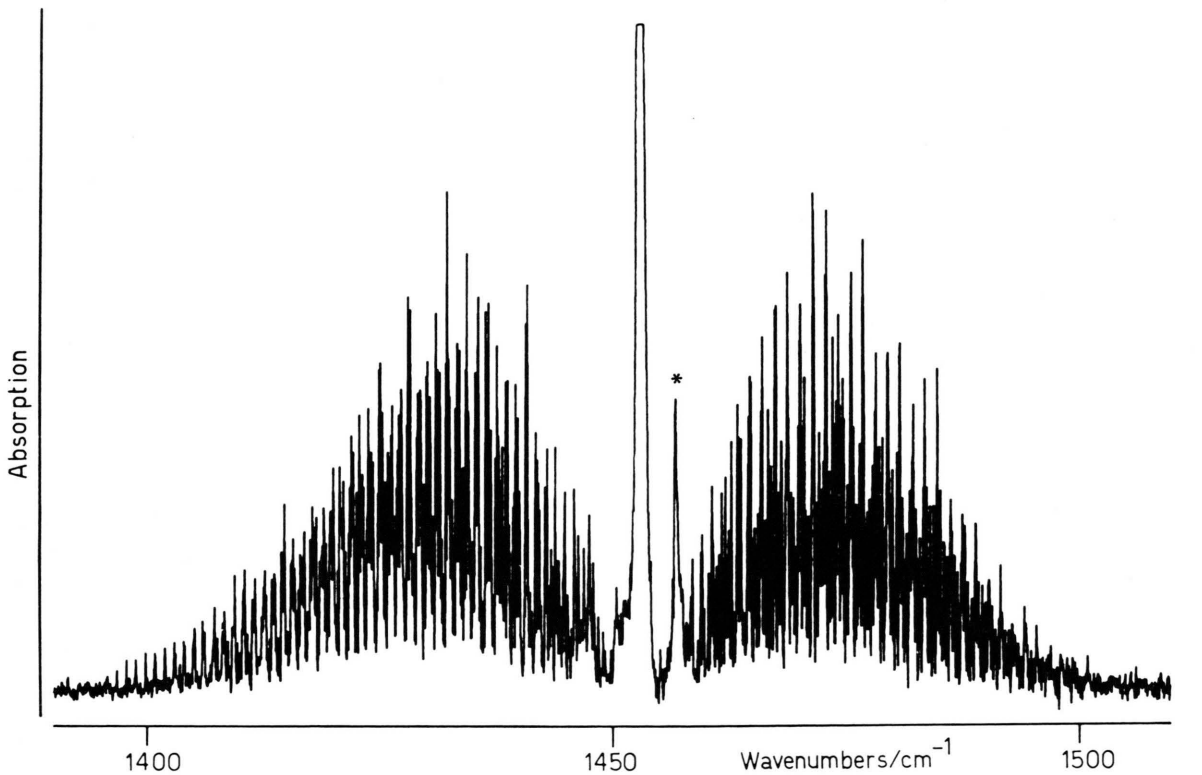

Fig. 3. The ν_3 band of diazirine, $H_2C^{15}N_2$. The asterisk indicates the Q-branch of the ν_3 fundamental of the isotopomer $H_2C^{14}N^{15}N$.

Table 2. Molecular constants in Watson's A-reduced Hamiltonian for the ν_3 fundamental of $H_2C^{15}N_2$.

	Ground state[a]	$\nu_3 = 1$
A/cm^{-1}	1.28772055	1.290252(98)[b]
B/cm^{-1}	0.773897232	0.771636(28)
C/cm^{-1}	0.536891243	0.5375082(53)
$\Delta_J \times 10^6$/cm^{-1}	1.00406	1.056(53)
$\Delta_{JK} \times 10^6$/cm^{-1}	3.3437	3.30(58)
$\Delta_K \times 10^6$/cm^{-1}	−0.8701	−0.8701[c]
$\delta_J \times 10^6$/cm^{-1}	0.309814	0.333(27)
$\delta_K \times 10^6$/cm^{-1}	2.45845	2.56(17)
$H_{JK} \times 10^{10}$/cm^{-1}	−0.2648	−0.2648[c]
$H_{KJ} \times 10^{10}$/cm^{-1}	0.749	0.749[c]
$\tilde{\nu}_0$/cm^{-1}	–	1452.4879(16)
σ/cm^{-1} (number of lines: 532)		0.014
$\varkappa$	−0.3687	−0.3779

[a] Ground state constants from [1] held fixed during the fit.
[b] Figures in parentheses are standard deviations in units of the least significant figures.
[c] Constrained to the ground state value during the fitting procedure.

the following selection rules were taken into account: $\Delta J = 0, \pm 1$, $\Delta K_a = 0$, $\Delta K_c = \pm 1$. The P, Q, and R branches are then each composed of subbranches designated by the notation $^{e,o}\Delta J\,(\Delta K_a, \Delta K_c)$, where e or o means that the sum of the three quantum numbers for the ground state is even or odd respectively, $^{e,o}P(0,1)$, $^{e}Q(0,1)$, $^{o}Q(0,-1)$, $^{e,o}R(0,1)$.

A first calculation of the rovibrational transition wavenumbers, together with the relative intensity of each line, was made using the ground state constants [1], for both states. Then, for each K_a, a correlation diagram was made of the deviation of the computed wavenumbers from the experimental positions of the peaks of the spectrum for increasing J' [13]. In each diagram it was possible to find a series of pairs of points for the P and R branch transitions going to the same excited rovibrational level. Since the differences observed between the P and R branch points depend only on the ground state constants which are very accurately determined from the

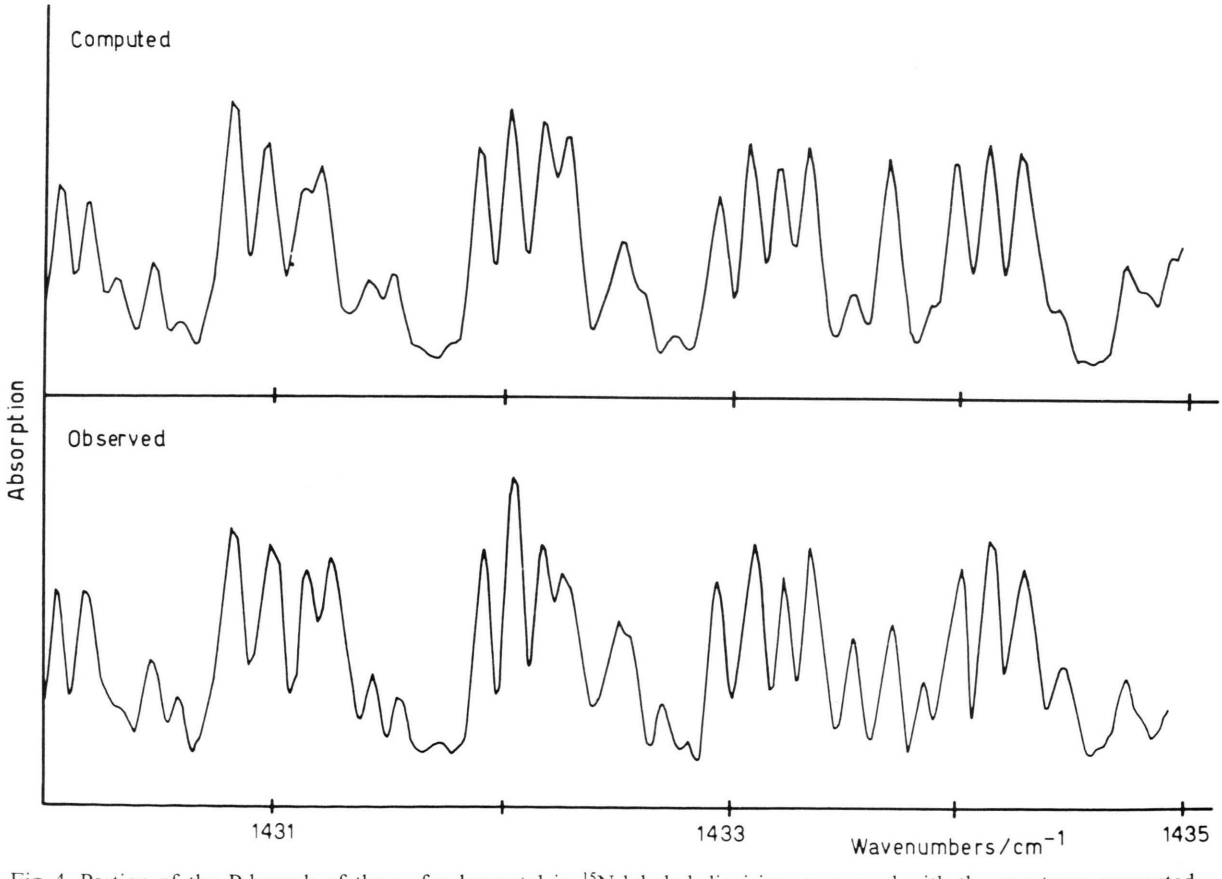

Fig. 4. Portion of the P-branch of the ν_3 fundamental in ^{15}N-labeled diazirine, compared with the spectrum computed with the adjusted constants reported in Table 2.

Table 3. Observed rovibrational transitions (wavenumbers/cm^{-1}) and assignment for the ν_3 fundamental of $^{15}N_2$-diazirine.

$J'(K'_a,K'_c)$-$J''(K''_a,K''_c)$	OBS	O-C	$J'(K'_a,K'_c)$-$J''(K''_a,K''_c)$	OBS	O-C	$J'(K'_a,K'_c)$-$J''(K''_a,K''_c)$	OBS	O-C
P-Branch			23(1,23)-24(1,24)	1426.608	-0.000	11(7, 4)-12(7, 5)	1436.218	-0.003
			23(0,23)-24(0,24)	1426.608	-0.000	12(2,10)-13(2,11)	1436.380	0.016
33(6,27)-34(6,28)	1410.344	0.006	22(2,21)-23(2,22)	1426.739	0.018	12(3,10)-13(3,11)	1436.380	-0.003
32(7,25)-33(7,26)	1410.344	-0.027	22(1,21)-23(1,22)	1426.739	0.018	10(5, 5)-11(5, 6)	1436.925	0.002
34(4,30)-35(4,31)	1411.273	-0.007	18(5,13)-19(5,14)	1427.000	0.019	13(0,13)-14(0,14)	1437.118	-0.004
31(7,24)-32(7,25)	1411.419	-0.001	22(1,22)-23(1,23)	1427.658	0.004	13(1,13)-14(1,14)	1437.118	-0.004
33(4,29)-34(4,30)	1412.343	0.018	22(0,22)-23(0,23)	1427.658	0.004	12(1,11)-13(1,12)	1437.286	0.002
31(6,25)-32(6,26)	1412.450	0.012	21(2,20)-22(2,21)	1427.756	-0.014	10(3, 7)-11(3, 8)	1437.286	0.010
30(7,23)-31(7,24)	1412.450	-0.018	21(1,20)-22(1,21)	1427.756	-0.014	12(2,11)-13(2,12)	1437.286	0.001
31(5,26)-32(5,27)	1413.447	0.013	16(6,10)-17(6,11)	1427.756	0.000	10(6, 4)-11(6, 5)	1437.430	-0.017
34(1,33)-35(1,34)	1414.205	-0.023	20(2,18)-21(2,19)	1427.892	-0.002	11(2, 9)-12(2,10)	1437.430	0.018
34(2,33)-35(2,34)	1414.205	-0.023	20(3,18)-21(3,19)	1427.892	-0.002	11(3, 9)-12(3,10)	1437.430	-0.028
29(6,23)-30(6,24)	1414.554	0.013	19(3,16)-20(3,17)	1428.003	-0.012	10(4, 7)-11(4, 8)	1437.826	-0.011
28(7,21)-29(7,22)	1414.554	-0.004	19(4,16)-20(4,17)	1428.003	-0.013	10(8, 3)-11(8, 4)	1437.826	0.001
34(0,34)-35(0,35)	1415.238	0.029	18(4,14)-19(4,15)	1428.111	0.007	10(8, 2)-11(8, 3)	1437.826	0.001
34(1,34)-35(1,35)	1415.238	0.029	18(5,14)-19(5,15)	1428.111	-0.015	9(4, 5)-10(4, 6)	1438.082	0.004
33(1,32)-34(1,33)	1415.238	-0.023	17(6,12)-18(6,13)	1428.317	0.004	12(1,12)-13(1,13)	1438.186	0.004
33(2,32)-34(2,33)	1415.238	-0.023	20(2,19)-21(2,20)	1428.838	0.015	12(0,12)-13(0,13)	1438.186	0.004
32(2,30)-33(2,31)	1415.347	0.023	20(1,19)-21(1,20)	1428.838	0.015	11(1,10)-12(1,11)	1438.369	0.022
32(3,30)-33(3,31)	1415.347	0.023	16(5,11)-17(5,12)	1428.838	-0.002	11(2,10)-12(2,11)	1438.369	0.020
30(4,26)-31(4,27)	1415.468	0.003	16(6,11)-17(6,12)	1429.467	-0.005	9(3, 6)-10(3, 7)	1438.369	0.006
28(6,22)-29(6,23)	1415.595	0.003	20(0,20)-21(0,21)	1429.762	0.013	10(3, 8)-11(3, 9)	1438.543	-0.001
27(7,20)-28(7,21)	1415.595	-0.001	15(7, 8)-16(7, 9)	1429.762	0.024	9(6, 4)-10(6, 5)	1438.968	-0.014
33(0,33)-34(0,34)	1416.219	-0.018	20(1,20)-21(1,21)	1429.762	0.013	9(6, 3)-10(6, 4)	1438.968	0.018
33(1,33)-34(1,34)	1416.219	-0.018	19(2,18)-20(2,19)	1429.864	-0.011	9(4, 6)-10(4, 7)	1439.087	0.016
27(6,21)-28(6,22)	1416.648	0.005	19(1,18)-20(1,19)	1429.864	-0.011	11(1,11)-12(1,12)	1439.228	-0.013
26(7,19)-27(7,20)	1416.648	0.024	18(2,16)-19(2,17)	1429.993	-0.014	11(0,11)-12(0,12)	1439.228	-0.013
32(0,32)-33(0,33)	1417.283	0.014	18(3,16)-19(3,17)	1429.993	-0.015	9(8, 2)-10(8, 3)	1439.228	-0.001
32(1,32)-33(1,33)	1417.283	0.014	17(3,14)-18(3,15)	1430.128	-0.004	9(8, 1)-10(8, 2)	1439.228	-0.001
26(6,20)-27(6,21)	1417.677	-0.015	17(4,14)-18(4,15)	1430.128	-0.008	9(2, 7)-10(2, 8)	1439.437	-0.017
31(1,31)-32(1,32)	1418.313	0.012	15(7, 9)-16(7,10)	1430.417	-0.018	10(2, 9)-11(2,10)	1439.437	0.022
31(0,31)-32(0,32)	1418.313	0.012	15(8, 7)-16(8, 8)	1430.417	-0.003	10(1, 9)-11(1,10)	1439.437	0.028
24(7,17)-25(7,18)	1418.584	-0.022	19(0,19)-20(0,20)	1430.773	-0.024	9(3, 7)-10(3, 8)	1439.647	-0.005
25(6,19)-26(6,20)	1418.738	-0.001	14(6, 8)-15(6, 9)	1430.773	0.017	8(5, 3)- 9(5, 4)	1440.195	0.023
29(1,28)-30(1,29)	1419.428	0.019	19(1,19)-20(1,20)	1430.773	-0.024	10(0,10)-11(0,11)	1440.311	0.008
29(2,28)-30(2,29)	1419.428	0.019	18(2,17)-19(2,18)	1430.939	0.008	10(1,10)-11(1,11)	1440.311	0.008
27(3,24)-28(3,25)	1419.560	-0.019	18(1,17)-19(1,18)	1430.939	0.008	8(5, 4)- 9(5, 5)	1440.311	0.008
27(4,24)-28(4,25)	1419.560	-0.019	17(3,15)-18(3,16)	1431.093	0.026	8(2, 6)- 9(2, 7)	1440.470	0.014
23(7,16)-24(7,17)	1419.560	0.025	17(2,15)-18(2,16)	1431.093	0.026	9(2, 8)-10(2, 9)	1440.470	-0.014
25(5,20)-26(5,21)	1419.758	0.009	16(3,13)-17(3,14)	1431.192	0.002	9(1, 8)-10(1, 9)	1440.470	0.001
24(6,18)-25(6,19)	1419.758	-0.022	16(4,13)-17(4,14)	1431.192	-0.006	8(3, 6)- 9(3, 7)	1440.783	-0.010
28(1,27)-29(1,28)	1420.422	-0.026	15(5,11)-16(5,12)	1431.375	0.006	7(3, 4)- 8(3, 5)	1440.964	-0.015
28(2,27)-29(2,28)	1420.422	-0.026	14(7, 7)-15(7, 8)	1431.496	0.006	9(0, 9)-10(0,10)	1441.372	0.006
22(7,15)-23(7,16)	1420.422	0.009	18(0,18)-19(0,19)	1431.863	0.014	9(1, 9)-10(1,10)	1441.372	0.006
26(3,23)-27(3,24)	1420.638	0.008	18(1,18)-19(1,19)	1431.863	0.014	8(2, 7)- 9(2, 8)	1441.535	-0.025
26(4,23)-27(4,24)	1420.638	0.008	14(7, 8)-15(7, 9)	1431.863	-0.003	8(1, 7)- 9(1, 8)	1441.535	0.012
24(5,19)-25(5,20)	1420.821	0.019	17(2,16)-18(2,17)	1431.984	-0.001	7(5, 2)- 8(5, 3)	1441.689	0.017
23(6,17)-24(6,18)	1420.821	0.010	14(6, 9)-15(6,10)	1431.984	0.022	7(4, 4)- 8(4, 5)	1441.689	-0.002
21(7,14)-22(7,15)	1421.251	-0.025	17(1,16)-18(1,17)	1431.984	-0.001	7(6, 2)- 8(6, 3)	1441.802	-0.017
28(1,28)-29(1,29)	1421.387	-0.018	14(8, 6)-15(8, 7)	1431.984	0.001	7(6, 1)- 8(6, 2)	1441.802	-0.015
27(1,26)-28(1,27)	1421.501	0.010	14(4,10)-15(4,11)	1432.116	0.011	7(3, 5)- 8(3, 6)	1441.964	-0.013
27(2,26)-28(2,27)	1421.501	0.010	16(3,14)-17(3,15)	1432.116	-0.010	8(0, 8)- 9(0, 9)	1442.428	-0.001
25(3,22)-26(3,23)	1421.676	-0.005	16(2,14)-17(2,15)	1432.116	-0.010	8(1, 8)- 9(1, 9)	1442.428	-0.002
25(4,22)-26(4,23)	1421.676	-0.005	14(5,10)-15(5,11)	1432.490	-0.005	6(2, 4)- 7(2, 5)	1442.646	-0.002
23(5,18)-24(5,19)	1421.843	-0.011	13(6, 7)-14(6, 8)	1432.490	0.023	7(2, 6)- 8(2, 7)	1442.646	-0.002
22(6,16)-23(6,17)	1421.843	0.021	17(1,17)-18(1,18)	1432.893	-0.007	6(4, 2)- 7(4, 3)	1442.891	0.000
20(7,13)-21(7,14)	1422.220	0.000	17(0,17)-18(0,18)	1432.893	-0.007	6(4, 3)- 7(4, 4)	1443.067	0.007
26(1,25)-27(1,26)	1422.513	-0.020	13(4, 9)-14(4,10)	1433.062	0.005	6(6, 1)- 7(6, 2)	1443.192	-0.019
26(2,25)-27(2,26)	1422.513	-0.020	16(1,15)-17(1,16)	1433.062	0.018	6(3, 4)- 7(3, 5)	1443.192	-0.019
25(2,23)-26(2,24)	1422.646	0.014	16(2,15)-17(2,16)	1433.062	0.018	6(6, 0)- 7(6, 1)	1443.192	-0.019
25(3,23)-26(3,24)	1422.646	0.014	15(2,13)-16(2,14)	1433.189	0.002	7(0, 7)- 8(0, 8)	1443.496	0.002
21(6,15)-22(6,16)	1422.801	0.001	15(3,13)-16(3,14)	1433.189	0.000	7(1, 7)- 8(1, 8)	1443.496	-0.000
26(1,26)-27(1,27)	1423.480	-0.002	14(3,11)-15(3,12)	1433.308	0.023	6(1, 5)- 7(1, 6)	1443.606	0.014
26(0,26)-27(0,27)	1423.480	-0.002	13(6, 8)-14(6, 9)	1433.308	0.010	6(2, 5)- 7(2, 6)	1443.742	-0.014
23(3,20)-24(3,21)	1423.763	-0.025	13(7, 7)-14(7, 8)	1433.308	-0.015	5(2, 3)- 6(2, 4)	1443.926	-0.008
23(4,20)-24(4,21)	1423.763	-0.025	13(8, 6)-14(8, 7)	1433.488	-0.018	5(3, 2)- 6(3, 3)	1444.070	0.022
21(5,16)-22(5,17)	1423.952	0.002	13(8, 5)-14(8, 6)	1433.488	-0.000	6(0, 6)- 7(0, 7)	1444.567	0.009
25(1,25)-26(1,26)	1424.519	-0.004	13(5, 9)-14(5,10)	1433.662	-0.004	6(1, 6)- 7(1, 7)	1444.567	0.001
25(0,25)-26(0,26)	1424.519	-0.004	16(1,16)-17(1,17)	1433.967	0.013	5(2, 4)- 6(2, 5)	1444.895	-0.001
24(1,23)-25(1,24)	1424.632	0.007	16(0,16)-17(0,17)	1433.967	0.013	4(2, 2)- 5(2, 3)	1445.364	0.027
24(2,23)-25(2,24)	1424.632	0.007	15(2,14)-16(2,15)	1434.095	-0.006	5(0, 5)- 6(0, 6)	1445.618	0.000
19(6,13)-20(6,14)	1424.632	0.004	12(4, 8)-13(4, 9)	1434.095	0.016	5(1, 5)- 6(1, 6)	1445.618	-0.022
23(2,21)-24(2,22)	1424.756	0.023	15(1,14)-16(1,15)	1434.095	-0.006	4(3, 1)- 5(3, 2)	1445.618	0.009
23(3,21)-24(3,22)	1424.756	0.023	14(2,12)-15(2,13)	1434.237	-0.010	4(3, 2)- 5(3, 3)	1445.817	0.001
19(8,12)-20(8,13)	1424.756	-0.017	14(3,12)-15(3,13)	1434.237	-0.013	4(4, 0)- 5(4, 1)	1445.817	0.002
21(4,17)-22(4,18)	1424.945	-0.000	13(4,10)-14(4,11)	1434.399	-0.019	4(4, 1)- 5(4, 2)	1445.817	-0.010
19(7,13)-20(7,14)	1425.233	-0.024	12(6, 7)-13(6, 8)	1434.698	0.013	4(2, 3)- 5(2, 4)	1446.089	0.012
18(8,10)-19(8,11)	1425.233	0.024	12(7, 5)-13(7, 6)	1434.698	-0.019	4(0, 4)- 5(0, 5)	1446.692	0.020
18(6,12)-19(6,13)	1425.538	0.002	15(0,15)-16(0,16)	1434.991	-0.017	3(2, 1)- 4(2, 2)	1446.806	-0.012
23(2,22)-24(2,23)	1425.648	-0.023	15(1,15)-16(1,16)	1434.991	-0.017	3(1, 2)- 4(1, 3)	1446.904	-0.021
23(1,22)-24(1,23)	1425.648	-0.023	12(8, 5)-13(8, 6)	1434.991	0.027	3(2, 2)- 4(2, 3)	1447.279	-0.021
22(2,20)-23(2,21)	1425.779	-0.006	13(2,11)-14(2,12)	1435.282	-0.025	3(0, 3)- 4(0, 4)	1447.715	-0.003
22(3,20)-23(3,21)	1425.779	-0.006	12(3, 9)-13(3,10)	1435.282	-0.025	3(1, 3)- 4(1, 4)	1447.823	-0.001
21(3,18)-22(3,19)	1425.896	-0.004	12(4, 9)-13(4,10)	1435.516	-0.005	2(1, 1)- 3(1, 2)	1448.261	0.018
21(4,18)-22(4,19)	1425.896	-0.004	11(6, 5)-12(6, 6)	1435.876	0.005	2(2, 1)- 3(2, 2)	1448.583	0.018
20(4,16)-21(4,17)	1426.017	0.015	14(1,14)-15(1,15)	1436.080	0.015	2(0, 2)- 3(0, 3)	1448.796	0.010
19(5,14)-20(5,15)	1426.017	0.018	14(0,14)-15(0,15)	1436.080	0.015	2(1, 2)- 3(1, 3)	1448.978	0.027
19(6,14)-20(6,15)	1426.136	0.029	13(2,12)-14(2,13)	1436.218	-0.004	1(1, 0)- 2(1, 1)	1449.634	0.004
18(8,11)-19(8,12)	1426.136	-0.019	13(1,12)-14(1,13)	1436.218	-0.004	0(0, 0)- 1(0, 1)	1451.192	0.014

Table 3 (continued)

$J'(K_a',K_c')-J''(K_a'',K_c'')$	OBS	O-C
R-Branch		
2(1, 2)- 1(1, 1)	1454.884	0.008
2(0, 2)- 1(0, 1)	1455.044	0.002
2(1, 1)- 1(1, 0)	1455.347	0.006
3(2, 2)- 2(2, 1)	1456.434	0.010
4(2, 3)- 3(2, 2)	1457.681	0.003
4(3, 2)- 3(3, 1)	1457.866	0.022
4(2, 2)- 3(2, 1)	1458.124	-0.009
5(0, 5)- 4(0, 4)	1458.301	-0.011
5(2, 4)- 4(2, 3)	1458.905	0.012
5(1, 4)- 4(1, 3)	1459.218	0.004
5(4, 2)- 4(4, 1)	1459.218	0.010
5(4, 1)- 4(4, 0)	1459.218	-0.001
6(1, 6)- 5(1, 5)	1459.362	0.004
6(0, 6)- 5(0, 5)	1459.362	-0.015
5(3, 2)- 4(3, 1)	1459.362	-0.000
5(2, 3)- 4(2, 2)	1459.580	-0.004
6(2, 5)- 5(2, 4)	1460.065	-0.000
6(1, 5)- 5(1, 4)	1460.316	0.008
7(1, 7)- 6(1, 6)	1460.443	0.000
7(0, 7)- 6(0, 6)	1460.443	-0.007
6(3, 4)- 5(3, 3)	1460.443	-0.026
6(2, 4)- 5(2, 3)	1460.960	0.005
7(2, 6)- 6(2, 5)	1461.208	0.005
7(1, 6)- 6(1, 5)	1461.344	-0.002
8(1, 8)- 7(1, 7)	1461.523	-0.002
8(0, 8)- 7(0, 7)	1461.523	-0.005
7(3, 5)- 6(3, 4)	1461.740	0.009
7(4, 4)- 6(4, 3)	1461.931	0.015
7(5, 3)- 6(5, 2)	1461.931	0.011
7(5, 2)- 6(5, 1)	1461.931	0.001
7(6, 2)- 6(6, 1)	1461.931	0.015
7(6, 1)- 6(6, 0)	1461.931	0.015
7(4, 3)- 6(4, 2)	1462.054	-0.012
9(0, 9)- 8(0, 8)	1462.605	-0.005
9(1, 9)- 8(1, 8)	1462.605	-0.004
8(3, 6)- 7(3, 5)	1462.955	0.008
8(4, 5)- 7(4, 4)	1463.269	0.021
8(5, 4)- 7(5, 3)	1463.269	-0.017
8(6, 3)- 7(6, 2)	1463.269	-0.000
8(6, 2)- 7(6, 1)	1463.269	-0.002
8(7, 2)- 7(7, 1)	1463.269	-0.005
8(7, 1)- 7(7, 0)	1463.269	-0.005
9(2, 8)- 8(2, 7)	1463.385	-0.022
8(2, 6)- 7(2, 5)	1463.385	0.027
8(4, 4)- 7(4, 3)	1463.569	-0.017
10(0,10)- 9(0, 9)	1463.685	-0.008
10(1,10)- 9(1, 9)	1463.685	-0.007
9(3, 7)- 8(3, 6)	1464.101	-0.016
10(1, 9)- 9(1, 8)	1464.533	0.026
9(4, 6)- 8(4, 5)	1464.533	-0.013
9(5, 5)- 8(5, 4)	1464.634	-0.019
9(6, 4)- 8(6, 3)	1464.634	-0.000
9(6, 3)- 8(6, 2)	1464.634	-0.008
9(7, 3)- 8(7, 2)	1464.634	0.010
9(7, 2)- 8(7, 1)	1464.634	0.010
9(8, 2)- 8(8, 1)	1464.634	-0.004
9(8, 1)- 8(8, 0)	1464.634	-0.004
11(0,11)-10(0,10)	1464.769	-0.008
9(5, 4)- 8(5, 3)	1464.769	0.002
11(1,11)-10(1,10)	1464.769	-0.008
9(3, 6)- 8(3, 5)	1465.189	0.013
10(2, 8)- 9(2, 7)	1465.418	0.002
11(2,10)-10(2, 9)	1465.575	-0.001
11(1,10)-10(1, 9)	1465.575	-0.006
12(0,12)-11(0,11)	1465.851	-0.012
12(1,12)-11(1,11)	1465.851	-0.012
10(5, 6)- 9(5, 5)	1465.983	-0.026
10(7, 4)- 9(7, 3)	1465.983	0.002
10(7, 3)- 9(7, 2)	1465.983	0.000
10(8, 3)- 9(8, 2)	1465.983	0.000
10(8, 2)- 9(8, 1)	1465.983	0.000
11(2, 9)-10(2, 8)	1466.421	-0.020
12(2,11)-11(2,10)	1466.652	-0.006
10(4, 6)- 9(4, 5)	1466.652	-0.005
12(1,11)-11(1,10)	1466.652	-0.008
13(1,13)-12(1,12)	1466.957	0.006
13(0,13)-12(0,12)	1466.957	0.006
11(5, 7)-10(5, 6)	1467.360	0.021
11(6, 6)-10(6, 5)	1467.360	-0.024
11(7, 5)-10(7, 4)	1467.360	0.011
11(7, 4)-10(7, 3)	1467.360	0.005
11(8, 4)-10(8, 3)	1467.360	0.026
11(8, 3)-10(8, 2)	1467.360	0.026
12(2,10)-11(2, 9)	1467.470	-0.017
12(3,10)-11(3, 9)	1467.470	0.018
11(3, 8)-10(3, 7)	1467.470	0.006
11(6, 5)-10(6, 4)	1467.470	0.004
13(2,12)-12(2,11)	1467.742	0.001
13(1,12)-12(1,11)	1467.742	0.000
14(0,14)-13(0,13)	1468.050	0.011
14(1,14)-13(1,13)	1468.050	0.011
11(4, 7)-10(4, 6)	1468.050	-0.025
13(2,11)-12(2,10)	1468.572	0.021
12(8, 5)-11(8, 4)	1468.689	-0.003
12(8, 4)-11(8, 3)	1468.689	-0.004
12(6, 7)-11(6, 6)	1468.784	0.028
15(1,15)-14(1,14)	1469.125	-0.002
15(0,15)-14(0,14)	1469.125	-0.002
12(4, 8)-11(4, 7)	1469.355	-0.006
14(2,12)-13(2,11)	1469.624	0.002
14(3,12)-13(3,11)	1469.624	0.008
13(5, 9)-12(5, 8)	1469.894	0.024
15(2,14)-14(2,13)	1469.894	-0.014
15(1,14)-14(1,13)	1469.894	-0.014
13(8, 6)-12(8, 5)	1470.055	-0.005
13(8, 5)-12(8, 4)	1470.055	-0.009
13(7, 6)-12(7, 5)	1470.174	0.010
14(3,11)-13(3,10)	1470.493	0.012
13(4, 9)-12(4, 8)	1470.493	-0.012
13(6, 7)-12(6, 6)	1470.493	-0.009
15(2,13)-14(2,12)	1470.684	-0.013
15(3,13)-14(3,12)	1470.684	-0.010
16(2,15)-15(2,14)	1470.995	0.000
16(1,15)-15(1,14)	1470.995	0.000
14(6, 9)-13(6, 8)	1471.414	-0.013
16(3,14)-15(3,13)	1471.770	-0.005
16(2,14)-15(2,13)	1471.770	-0.006
14(6, 8)-13(6, 7)	1472.076	-0.019
17(2,16)-16(2,15)	1472.076	-0.004
17(1,16)-16(1,15)	1472.076	-0.004
15(5,11)-14(5,10)	1472.232	0.020
18(1,18)-17(1,17)	1472.418	0.016
18(0,18)-17(0,17)	1472.418	0.016
16(3,13)-15(3,12)	1472.554	-0.025
16(4,13)-15(4,12)	1472.554	-0.009
17(3,15)-16(3,14)	1472.834	-0.022
17(2,15)-16(2,14)	1472.834	-0.023
15(7, 9)-14(7, 8)	1472.834	-0.022
15(8, 8)-14(8, 7)	1472.834	0.013
18(1,17)-17(1,16)	1473.158	-0.010
15(7, 8)-14(7, 7)	1473.158	0.005
18(2,17)-17(2,16)	1473.158	-0.010
16(5,12)-15(5,11)	1473.326	-0.001
16(4,12)-15(4,11)	1473.502	0.012
19(1,19)-18(1,18)	1473.502	0.007
15(5,10)-14(5, 9)	1473.502	-0.001
19(0,19)-18(0,18)	1473.502	0.007
17(3,14)-16(3,13)	1473.634	-0.013
17(4,14)-16(4,13)	1473.634	-0.006
15(6, 9)-14(6, 8)	1473.634	-0.026
18(3,16)-17(3,15)	1473.933	-0.006
16(6,11)-15(6,10)	1473.933	0.005
18(2,16)-17(2,15)	1473.933	-0.006
16(8, 9)-15(8, 8)	1474.210	0.003
16(7,10)-15(7, 9)	1474.226	0.025
20(0,20)-19(0,19)	1474.586	-0.002
16(5,11)-15(5,10)	1474.586	0.002
20(1,20)-19(1,19)	1474.586	-0.002
18(3,15)-17(3,14)	1474.711	-0.009
18(4,15)-17(4,14)	1474.711	-0.006
19(3,17)-18(3,16)	1475.034	0.010
19(2,17)-18(2,16)	1475.034	0.010
17(6,12)-16(6,11)	1475.122	0.018
16(6,10)-15(6, 9)	1475.122	0.000
18(4,14)-17(4,13)	1475.529	-0.010
18(5,14)-17(5,13)	1475.529	0.027
17(7,11)-16(7,10)	1475.529	0.024
21(1,21)-20(1,20)	1475.672	-0.012
21(0,21)-20(0,20)	1475.672	-0.012
19(3,16)-18(3,15)	1475.791	-0.005
17(8, 9)-16(8, 8)	1475.791	-0.007
20(3,18)-19(3,17)	1476.097	-0.010
20(2,18)-19(2,17)	1476.097	-0.010
18(6,13)-17(6,12)	1476.221	-0.017
21(1,20)-20(1,19)	1476.452	0.013
17(6,11)-16(6,10)	1476.452	0.014
21(2,20)-20(2,19)	1476.452	0.013
19(5,15)-18(5,14)	1476.580	0.002
19(4,15)-18(4,14)	1476.580	-0.013
21(3,19)-20(3,18)	1477.186	-0.007
21(2,19)-20(2,18)	1477.186	-0.007
19(6,14)-18(6,13)	1477.359	0.015
18(8,10)-17(8, 9)	1477.359	-0.002
22(1,21)-21(1,20)	1477.546	0.016
22(2,21)-21(2,20)	1477.546	0.016
20(4,16)-19(4,15)	1477.650	-0.007
20(5,16)-19(5,15)	1477.650	-0.000
22(2,20)-21(2,19)	1478.260	-0.020
22(3,20)-21(3,19)	1478.260	-0.020
19(8,12)-18(8,11)	1478.260	-0.016
20(6,15)-19(6,14)	1478.437	0.008
19(6,13)-18(6,12)	1478.631	0.014
23(1,22)-22(1,21)	1478.631	0.008
23(2,22)-22(2,21)	1478.631	0.008
21(5,17)-20(5,16)	1478.736	0.011
21(4,17)-20(4,16)	1478.736	0.009
24(1,24)-23(1,23)	1478.991	0.014
24(0,24)-23(0,23)	1478.991	0.014
19(8,11)-18(8,10)	1478.991	0.017
23(2,21)-22(2,20)	1479.354	-0.014
23(3,21)-22(3,20)	1479.354	-0.014
21(6,16)-20(6,15)	1479.521	0.017
21(5,16)-20(5,15)	1479.521	-0.016
24(2,23)-23(2,22)	1479.699	-0.017
24(1,23)-23(1,22)	1479.699	-0.017
25(1,25)-24(1,24)	1480.081	0.005
25(0,25)-24(0,24)	1480.081	0.005
21(7,15)-20(7,14)	1480.249	0.002
22(6,17)-21(6,16)	1480.558	-0.015
20(7,13)-19(7,12)	1480.558	0.010
20(8,12)-19(8,11)	1480.558	-0.012
25(1,24)-24(1,23)	1480.834	0.022
25(2,24)-24(2,23)	1480.834	0.022
26(1,26)-25(1,25)	1481.173	-0.002
26(0,26)-25(0,25)	1481.173	-0.002
22(7,16)-21(7,15)	1481.335	-0.004
25(3,23)-24(3,22)	1481.549	0.000
25(2,23)-24(2,22)	1481.549	0.000
23(6,18)-22(6,17)	1481.624	-0.018
23(5,18)-22(5,17)	1481.624	-0.024
24(5,20)-23(5,19)	1481.941	-0.011
24(4,20)-23(4,19)	1481.941	-0.011
27(1,27)-26(1,26)	1482.295	0.017
27(0,27)-26(0,26)	1482.295	0.017
26(3,24)-25(3,23)	1482.617	-0.022
26(2,24)-25(2,23)	1482.617	-0.022
25(5,21)-24(5,20)	1483.028	-0.002
27(1,26)-26(1,25)	1483.028	0.024
27(2,26)-26(2,25)	1483.028	0.024
25(4,21)-24(4,20)	1483.028	-0.002
28(1,28)-27(1,27)	1483.398	0.018
28(0,28)-27(0,27)	1483.398	0.018
24(6,18)-23(6,17)	1483.517	0.001
27(3,25)-26(3,24)	1483.745	0.014
27(2,25)-26(2,24)	1483.745	0.014
28(2,27)-27(2,26)	1484.115	0.013
28(1,27)-27(1,26)	1484.115	0.013
26(5,22)-25(5,21)	1484.115	0.004
26(4,22)-25(4,21)	1484.115	0.004
29(1,29)-28(1,28)	1484.481	-0.001
29(0,29)-28(0,28)	1484.481	-0.001
25(6,19)-24(6,18)	1484.581	0.017
28(2,26)-27(2,25)	1484.840	0.016
26(6,21)-25(6,20)	1484.840	-0.015
26(5,21)-25(5,20)	1484.840	-0.016
29(2,28)-28(2,27)	1485.196	-0.003
27(5,23)-26(5,22)	1485.196	0.004
27(4,23)-26(4,22)	1485.196	0.004
29(1,28)-28(1,27)	1485.196	-0.003
26(7,20)-25(7,19)	1485.586	-0.028
30(0,30)-29(0,29)	1485.586	-0.000
30(1,30)-29(1,29)	1485.586	-0.000
27(5,22)-26(5,21)	1485.926	-0.004
27(6,22)-26(6,21)	1485.926	-0.004
30(1,29)-29(1,28)	1486.277	-0.022
28(5,24)-27(5,23)	1486.277	0.003
28(4,24)-27(4,23)	1486.277	0.003
31(0,31)-30(0,30)	1486.671	-0.020
27(7,21)-26(7,20)	1486.671	-0.008
31(1,31)-30(1,30)	1486.671	-0.020
27(6,21)-26(6,20)	1486.671	-0.011
28(6,23)-27(6,22)	1487.008	0.002
28(5,23)-27(5,22)	1487.008	0.002
29(4,25)-28(4,24)	1487.385	0.027
31(2,30)-30(2,29)	1487.385	-0.014
31(1,30)-30(1,29)	1487.385	-0.014
28(6,22)-27(6,21)	1487.747	-0.001
28(7,22)-27(7,21)	1487.747	-0.000
29(6,24)-28(6,23)	1488.088	0.005
29(5,24)-28(5,23)	1488.088	0.005
32(2,31)-31(2,30)	1488.490	-0.010
32(1,31)-31(1,30)	1488.490	-0.010
30(6,25)-29(6,24)	1489.166	0.005
30(5,25)-29(5,24)	1489.166	0.005
33(2,32)-32(2,31)	1489.583	-0.019
32(4,28)-31(4,27)	1490.634	0.021
32(5,28)-31(5,27)	1490.634	0.021

microwave data [1], these lines could be unambiguously assigned.

Keeping the molecular constants for the ground state fixed, the constants for the level $v_3 = 1$ were refined by the least-squares method and the above procedure repeated with successively larger sets of assigned transitions. At each step of the assignment procedure, the experimental spectrum was compared with the computed one, obtained by a Lorentz line-shape function convoluted with a rectangular line shape function and adjusting thereby with the experimental parameters.

In Table 2, the molecular constants obtained from the least-squares analysis of more than 500 assigned transitions are reported. The standard deviation of the fit ($0.014\,cm^{-1}$) is compatible with the resolution of the spectrum. The assignment of the transitions was completed up to $K_a = 8$ and $J = 35$. Due to the medium resolution of the spectrum, the quartic constant Δ_K and the sextic centrifugal distortion constants could not be included in the least-squares analysis.

Table 3 reports the observed values of the assigned transitions included in the fitting procedure together with the difference between these values and those computed from the adjusted constants of Table 2. The difference between the observed and calculated line positions is consistent with the instrumental resolution. A part of the spectrum in the P branch region of the ν_3 band compared with the computed spectrum is shown in Figure 4. Considering the fact that the ν_3 band of $H_2C^{14}N^{15}N$ and no hot bands of $H_2C^{15}N_2$ have been taken into account the computed spectrum simulates the observed one very well.

The determination of the rotational and centrifugal distortion constants for the first vibrational state of the methylene bending fundamental in $^{15}N_2$-diazirine has confirmed the validity of the methods developed for the analysis of this asymmetric top molecule. The extension of the investigation to the other fundamental modes of diazirine and its isotopomers will give a complete representation of these molecules in their vibrational states. The molecular parameters obtained from these analyses will be also helpful for the determination of the molecular force field in the normal coordinate analysis of diazirine [11].

Acknowledgements

The authors would like to express their thanks to Prof. Dr. Manfred Winnewisser for stimulating discussions and Dr. Brenda P. Winnewisser for critically reading the manuscript. The experimental work was supported by funds of Deutsche Forschungsgemeinschaft and the Fonds der chemischen Industrie. Calculations were carried out at the Hochschulrechenzentrum of the Justus Liebig University of Giessen.

[1] J. Vogt, M. Winnewisser, and J. J. Christiansen, J. Mol. Spectrosc. **103,** 95 (1984).
[2] M. Bogey, M. Winnewisser, and J. J. Christiansen, Can. J. Phys. **62,** 1198 (1984).
[3] K. Möller, J. Vogt, M. Winnewisser, and J. J. Christiansen, Can. J. Phys. **62,** 1217 (1984).
[4] U. P. Verma, K. Möller, J. Vogt, M. Winnewisser, and J. J. Christiansen, Can. J. Phys. **63,** 1173 (1985).
[5] A. Gambi, M. Winnewisser, and J. J. Christiansen, J. Mol. Spectrosc. **98,** 413 (1983).
[6] A. Gambi, J. Mol. Spectrosc. **103,** 321 (1984).
[7] A. Gambi, U. P. Verma, M. Winnewisser, and G. Guelachvili, J. Mol. Spectrosc. **108,** 264 (1984).
[8] A. Gambi, M. Pedrali, M. Winnewisser, and G. Guelachvili, J. Mol. Spectrosc. **113,** 250 (1985).
[9] R. Ohme and E. Schmitz, Chem. Ber. **97,** 297 (1964).
[10] A. R. H. Cole (Ed.), IUPAC Table of Wavenumbers for the Calibration of Infrared Spectrometers, 2nd ed. Pergamon Press, Oxford 1977.
[11] B. P. Winnewisser and A. Gambi, to be published.
[12] J. K. G. Watson, in "Vibrational Spectra and Structure" (J. R. Durig, Ed.), Vol. 6, Elsevier, Amsterdam 1977.
[13] T. Nakagawa and J. Overend, J. Mol. Spectrosc. **50,** 333 (1974).